Entrainment coefficient and Coanda bubble plume flows

Daniel G. Duarte*
Maria Helena Farias†
Rodrigo P. de Oliveira*
Atila P. Silva Freire*

†Diretoria de Metrologia Científica, Inmetro, Duque de Caxias, 22050-050, Brasil
*PEM/COPPE/UFRJ, C.P. 68503, 21945-970, Rio de Janeiro, Brasil

Abstract. *The present work uses particle image velocimetry (PIV) to assess the entrainment coefficient (λ) behaviour in plumes that are set to develop close to a wall. When that happens, the plume is observed to bend toward the wall, due to a physical process that is here speculated to be provoked by an inhibition of the entrainment coefficient. A reduction in λ of about 10% should provoke a deflection of the plume of about 6 degrees. Mean velocity, void fraction and turbulence profiles are presented.*

Keywords: *Bubble plume, Coanda effect, PIV.*

1. Introduction

The injection of bubbles into a liquid environment serves to many purposes in industry. Chemical reactors and gas stirred melt ladles are typical examples. While in reactors the achievement of a large interfacial area is the primary target, in gas stirring operations one seeks to achieve the maximum possible liquid metal homogenization in the minimum time.

The present work deals with a physical phenomenon that is typical of the steel making industry, that is, the insertion of an inert gas into a reservoir filled with a stagnant fluid. In particular, the degree of agitation provoked by the bubbles must be such as to achieve minimum mixing times and maximum recoveries of alloy additions at optimum flow rates. This naturally raises the question: what is the best way to inject gas in a vessel with molten metal. Usual configurations include a single gas plume, a combination of geometrically arranged plumes or a curtain of bubbles.

Many works in literature tackle the problem of axisymmetric bubble plumes. However, in industrial applications gas is many times injected at positions prone to be affected by wall proximity. Under this condition, a strong three dimensional flow configuration will develop. The result is that mixing times cannot be related directly to the stirring energy input through a simple power law. Further conditions including vessel geometry and the location and rate of gas injection have to be considered.

Mazumdar and Guthrie(1995) have noted that eddy diffusion and bulk convection play an important and almost equal role in the control of mixing in gas injection ladle operations. Other authors, Asai et al. (1983), Kim et al. (1987) and Dobson and Robertson (1986), have reported that mixing times decrease as the gas injector is located off-center. This observation is in contrast with Majurama et al. (1984) that have reported an increase in mixing times when gas is injected at the mid-radius of the vessel where wall effects and stagnation zones can be minimized.

The numerical modelling of gas stirring ladles was studied by Joo and Guthrie (1992) for operations that included single- or dual-injection bubbling procedures. In this work, single and double gas plume arrangements were investigated, with a series of porous plugs being located at center, one-third, half, and two-thirds radii. To validate the results some simple experiments were conducted to measure the mixing times against radial position. Basically a a tracer technique was used. The flow pattern for each arrangement was then numerically simulated with the help of a κ-ϵ turbulence model. In all numerical calculations, the plumes presented a clear upright position, irrespective of their proximity to the wall. Thus, no sign of the natural lateral distortion that plumes suffer when subject to wall effects was observed in the numerical computations. Some pictures of the phenomenon, taken by the same author, were however very clear in exhibiting the plume's lateral deflection. The mathematical modelling of the flow was, therefore, in clear disagreement with the experimental evidence. In this simulation, the action of the bubbles was limited only to the buoyancy term, resulting in a very simple model for the gas phase that could not predict the interaction between the plumes.

The purpose of the work is to investigate experimentally the behaviour that a bubble plume set to develop close to a wall will develop. When a bubble plumes is arranged in this geometry, it develops a tendency to cling to the vertical wall that is near to the orifice from which the gas emerges; this phenomenon is normally referred to in literature as the *Coanda effect*. This denomination has also been widely used to describe the atraction effects that flows issuing from adjacent orifices exert on each other. Here, we intend to show that the plume distortion is provoked by an inhibition of fluid entrainment by the mean flow.

In many situations, bubble plumes can be described through the two-dimensional continuity and momentum equations, expressed in cylindrical polar coordinates. As we have mentioned before, while many flows can be thought as having an axisymmetric form, a major feature of industrial flows is their three dimensional character. This feature is much enhanced

when the source of gas is located close to a wall or close to another source, so that the Coanda effect sets in. The present work follows Siva Freire et al. (2002) in trying to shown the usefulness of a simple integral formulation to capture all relevant features of the flow. The theory is an extension of the procedure of Ditmars and Cederwall (1974), making use, for the sake of simplicity, of Gaussian profiles and of Boussinesq assumption. The theory makes simple considerations about the conservation of the entrained momentum and proposes a new expression for the description of the entrainment coefficient as a function of the Weber number. Our primary purpose here is to show thorough PIV results that the hypothesis of entrainment inhibition is plausible. Here we will consider that the deflection of the plume is small enough so that integral theories can still be applied to the problem.

The single bubble plume flow has been extensively studied both theoretically (Ditmars and Cederwall (1974), Milgram (1983), Brevik and Killie (1996)) and experimentally ((Milgram(1983), Castillejos and Brimacombe(1987), Barbosa(1996)) by many authors in the past three decades. The studies cover a large range of conditions but fail to propose a single model capable of dealing with all possible variations in flow conditions. For the integral approaches, the flow has been divided into three distinct regions where some dominant effects prevail (Milgram (1983)). The buoyancy dominated region is normally referred to as the "Zone of Established Flow".

As far as the interaction between adjacent bubble plumes is concerned, no analysis (experimental or theoretical) has been identified by the present authors in literature. The interaction between laminar thermal plumes has been studied using a Mach-Zehnder interferometer (Pera and Gebhart (1975)). For this case, a simple model was developed in order to take into account the deflection angle of the centre lines of the plumes. Pera and Gebhart observed that plane plumes manifest stronger centre line inclinations than axisymmetric plumes.

Arrangements consisting of a single plume developing near to a wall where studied by Menut et al.(1998). This geometry classically defines the Coanda effect; in fact, when Weber and Froude numbers based on the distance between the gas source and the wall were high Menut et al. showed the plume to exhibit a type of a Coanda effect, bending towards the wall. The angle of deflection was observed to be about 2 degrees.

2. The Coanda effect

The definition of the Coanda effect has been clearly stated by Reba(1966) as

"The Coanda Effect is the tendency of a fluid, either gaseous or liquid, to cling to a vertical surface that is near to an orifice from which the fluid emerges".

An experimental fact is that when two point sources of buoyancy (or momentum) are placed side by side, the two resulting turbulent plumes (or jets) tend to bent towards each other.

For laminar flow, the deflection of the plumes normally results from pressure differences (Pera and Gebhart (1975)). For turbulent flows, on the other hand, the entrained fluid must must have a commanding effect on the flow properties. In axisymmetric geometries, the role played by pressure differences must be negligible since the net forces cancel out due to symmetry.

In the present work, we will shown how a simple model that considers the entrainment coefficient to vary along the periphery of the plume is capable to provide a good prediction of the plume deflection.

3. Experimental setup and flow instrumentation

The experimental apparatus is shown in Fig. 1. It comprises a water tank, an air injection system, a TSI 3D PIV data acquisition and analysis system. The glass water tank has dimensions 1x1x1 meter. The air injection system is composed of a mass flow meter and an injection nozzles with a single 3.2 mm diameter hole. The data acquisition and analysis system consists of a microcomputer with an interface data acquisition board.

The water depth is kept constant and equal to 0.85 m. Approximately 15 minutes of continuous gas flow are necessary to guarantee a steady-state condition. Measurements of the bubble plume properties were made for a gas flow rate of 1 l/min. For the three dimensional plume, the gas plug was located at 45 mm away from the wall (Y = 45 mm, X =0, Z= 0).

4. Particle image velocimetry - PIV

In particle image velocimetry (PIV) small tracer particles are added to the flow. Then, provided the displacements of these particles can be tracked in space and time, the general dynamical features of the flow can be determined. In a typical procedure, the particles are successively illuminated in a plane within a short time interval. The light scattered by them is then recorded on separate frames on a CCD sensor. To determine the local displacement vectors, the recordings are split into small sub-areas termed *interrogation windows*. Then by considering the particles to have moved homogeneously between two consecutive exposition times, statistical methods can be used to find the displacements. The great advantages of PIV are its non-intrusive character and the large spatial resolution.

In two-phase flow applications, the information conveyed by each phase needs to be adequately separated. Hassan et al. (1998) have shown how PIV measurements in conjunction with a forward-projection shadow method can be used

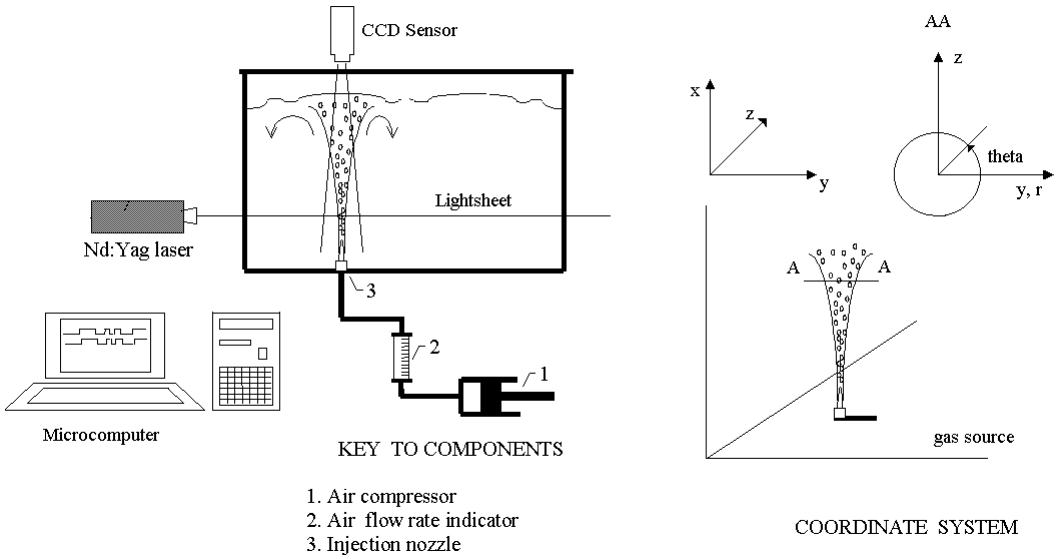

Figure 1. Experimental rig and sketch of PIV system.

to find the sizes and velocities of bubbles rising in a vertical pipes. Their experimental arrangement also allowed for an investigation of the dynamic properties of the continuous phase.

Lindken et al. (1999) showed that the application of filtering techniques to separate the signals resulting from both phases permits a high resolution of velocity measurements in regions near to interfaces.

Stereoscopic PIV uses two cameras to to investigate a flow field from two persperctives so that the out of plane velocity component can be evaluated. The two components of velocity orthogonal to the camera optical axis are measured from each camera perspective. The pair of two-dimensional velocity vectors is then combined to construct a three-dimensional velocity field. The two images are calibrated using a calibration target to map the locations between the flow and the cameras and also for the local magnifications in all three directions. The mapping function corrects the center of the field of views for the two cameras. it also accounts for image distortion. In this work we have used the Model 640050 stereo camera PIV system supplied by TSI.

To investigate the velocity field of the continuous phase, the water was seeded with a commonly used particle tracer, rodamim, 10 μm in size. The light source was furnished by two Nd:YAG lasers that produced short duration (10 ns) high energy (200 mJ) pulses of light green (532 nm). The collimated laser beam was transmitted through a cylindrical (15 mm) and a spherical (500 mm) lens generate a 1 mm thick lightsheet. The viewing velocity field was 30x30 cm, the interrogation window was defined with 32x64 pixes. The reflected light was recorded with two 6300059 Power View Plus 4 Megapixels CCD cameras (2048x2048 pixels at 8 Hz). The cameras were fitted with Nikkor 50 mm f/2.8D lens.

During normal operation, bubbles will cross the light sheet provoking large reflections that will hit directly the camera. Moderate disturbances can be corrected by passage of filtering techniques. The digital recordings were evaluated through a minimum quadratic difference method. The signals from the two phases were separated naturally due to the fluorescent character of the tracers. Basically the reflected signals were recorded with the help of an optical high pass filter. The shapes and positions of the bubbles were found from their shadows.

5. Measurements

Before measurements on a three dimensional bubble were performed, preliminary measurements on an axisymmetric bubble plume were made. The gas plug was placed at the tank center point; the gas flow rates was then set to 1 l/min.

The topography of the axisymmetric bubble plume is shown in Fig. 2 for measurements taken at three different planes located at distances of 235, 335 and 470 mm from the gas source. The spread of the velocity field with height is clearly seen. The Gaussian nature of the axisymmetric plume is further observed in Fig. 3. This is strong support for the establishment of an integral theory for the description of the phenomenon.

Mean-flow theories for bubble plumes are integral theories for which the forms of the radial distributions of the velocity and of the density deficiency between the plume and the surrounding fluid are considered to be known in advance. In fact, since the pioneering work of Kobus(1968) to the more recent theories, very little in terms of the formulation has changed. The recent theories have incorporated many novelties, but the basic formulation of the problem remains the same; the governing equations are constructed from the conditions of conservation of gas, conservation of liquid, and the change of momentum flux with buoyancy.

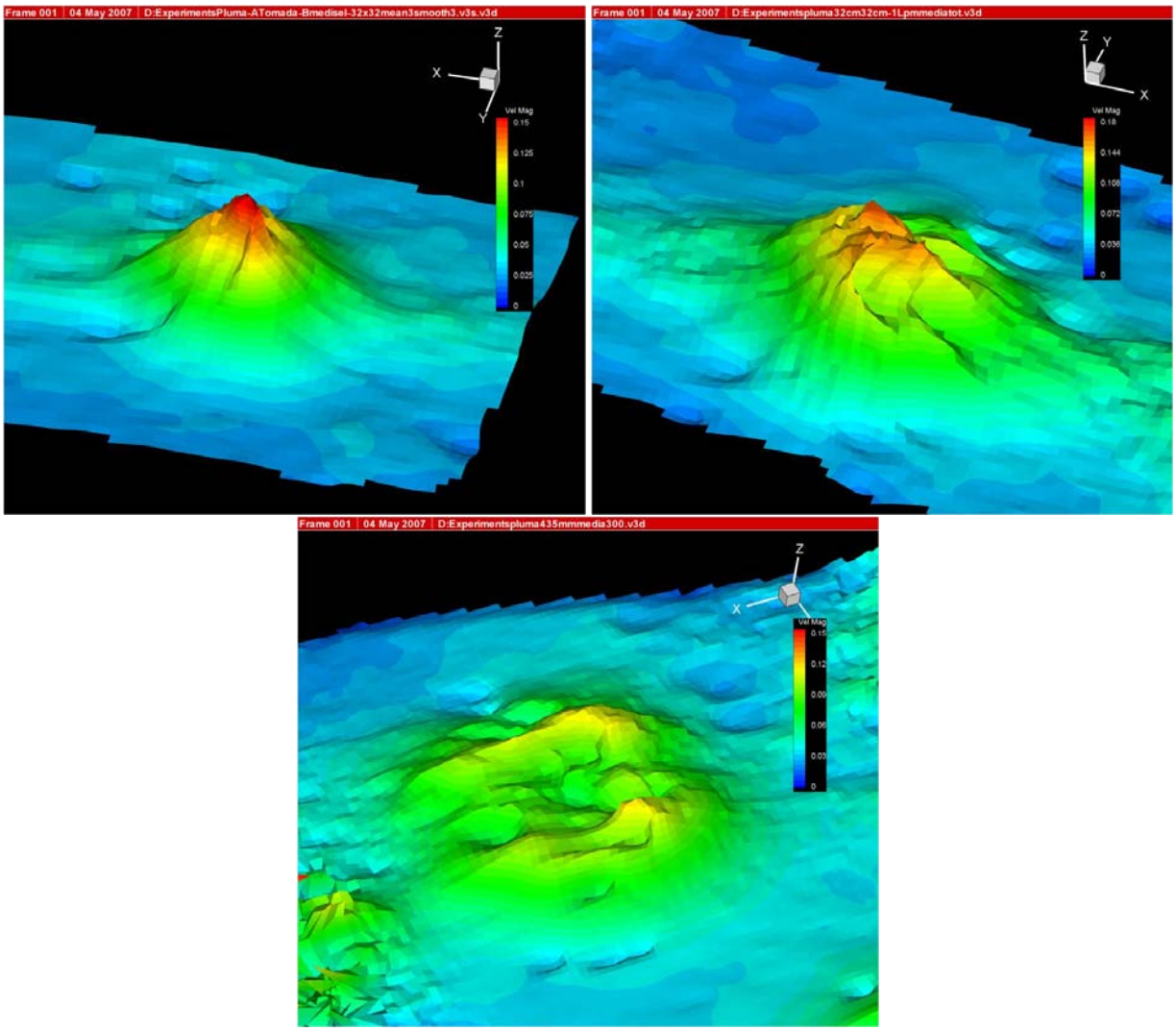

Figure 2. Flow topography of the axisymmetric bubble plume at stations 235, 335 and 470 mm respectively.

In the present work, the theory of Silva Freire et al. (2002) will be used as the basis for our developments. By allowing the entrainment coefficient to vary along the plume periphery, the effect of deflection provoked by an adjacent twin plume was conveniently modelled. This a very simple premise, which yields very good results.

Since the basic details of the theory can be found in Ditmars and Cederwall(1974), only a brief mention of them will be made here.

The velocity and mean density defect are given by

$$u(x,r) = u_m(x)\, e^{-r^2/b^2}, \tag{1}$$

$$\rho_a - \rho_m(x) = \Delta\rho_m(x)\, e^{-r^2/(\lambda b)^2}, \tag{2}$$

where $b(x)$ is the lateral dimension of the plume, ρ_a is the water density and λ is the lateral spread of density deficiency to momentum.

The liquid volume at any elevation and the momentum flux are given respectively by

$$Q = \int_0^\infty 2\,\pi\, u\, r\, dr = \pi u_m b^2, \text{ and} \tag{3}$$

$$M = \int_0^\infty 2\,\pi\, \rho_a\, u^2\, r\, dr = \frac{\pi}{2}\rho_a u_m^2 b^2. \tag{4}$$

The entrainment assumption is now taken as the explicit starting point of our theory, i.e., it is considered that the inflow velocity at the periphery of the plume is a fraction $\alpha(\theta)$ of the maximum plume centreline velocity according to

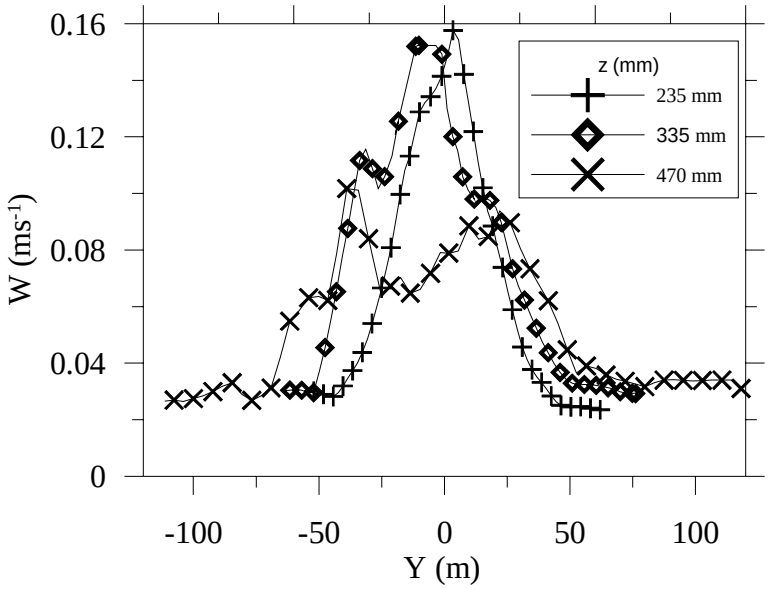

Figure 3. Gaussian nature of the axisymmetric plume at stations 235, 335 and 470 mm respectively.

$$\frac{dQ}{dx} = \int_0^{2\pi} \alpha(\theta)\, u_m\, b\, d\theta = \alpha_{int}\, (u_m\, b). \tag{5}$$

Then, using Boussinesq approximation, the equations of conservation of mass, x-momentum and buoyancy can be written as

$$\frac{d(\pi u_m b^2)}{dx} = \alpha_{int}\, (u_m\, b). \tag{6}$$

$$\frac{d(\pi u_m^2 b^2)}{dx} = \frac{2 g q_0 H_0}{(H_0 + H - x)(u_m(1+\lambda^2)^{-1} + u_b)}, \tag{7}$$

$$\pi \Delta\rho_m \lambda^2 b^2 \Big(\frac{u_m}{1+\lambda^2} + u_b\Big) = \frac{\rho_a q_0 H_0}{(H_0 + H - x)}. \tag{8}$$

Now, we consider that the bending of the plume is primarily due to an inhibition of the entrainment coefficient in the part of the plume which is nearer to the other. We also consider that all transversal momentum entrained in the plume is retained by its elements as they rise. If M_c denotes the transversal entrained momentum, then

$$M_c = \int_0^x \int_0^{2\pi} \rho_a\, (\alpha(\theta) u_m b)\, \alpha(\theta) u_m\, cos(\theta)\, d\theta dx, \tag{9}$$

and the plume deflection angle can be approximated by $\tan(\phi) = M_c/M$.

In Silva Freire et al. (2002), $\alpha(\theta)$ has been approximated by

$$\alpha(\theta) = \frac{\alpha_{max} - \alpha_{min}}{\pi}\theta + \alpha_{min},\ 0 < \theta < \pi \tag{10}$$

$$\alpha_{min} = 0.06 - 1.15\, W_e, \quad \alpha_{max} = 0.065. \tag{11}$$

Thus, Silva Freire et al. (2002) have proposed a very simple linear correlation for the prediction of the entrainment coefficient behaviour that needs to be validated by experimental data. In their original work, Silva Freire et al. (2002) used void fraction profiles to validate the proposed expressions. At the time, the authors did not have access to measuring techniques that could furnish them data on the liquid phase. In the present work we show how PIV data give information that is consistent with the results found in 2002.

The entrained velocities for the axisymmetric plume are shown in Figs. 4 and 5. Note that, as expected, the entrained flow is symmetric around the center of the plume and that, as stated by Eq. (5), its value is proportional do the plume

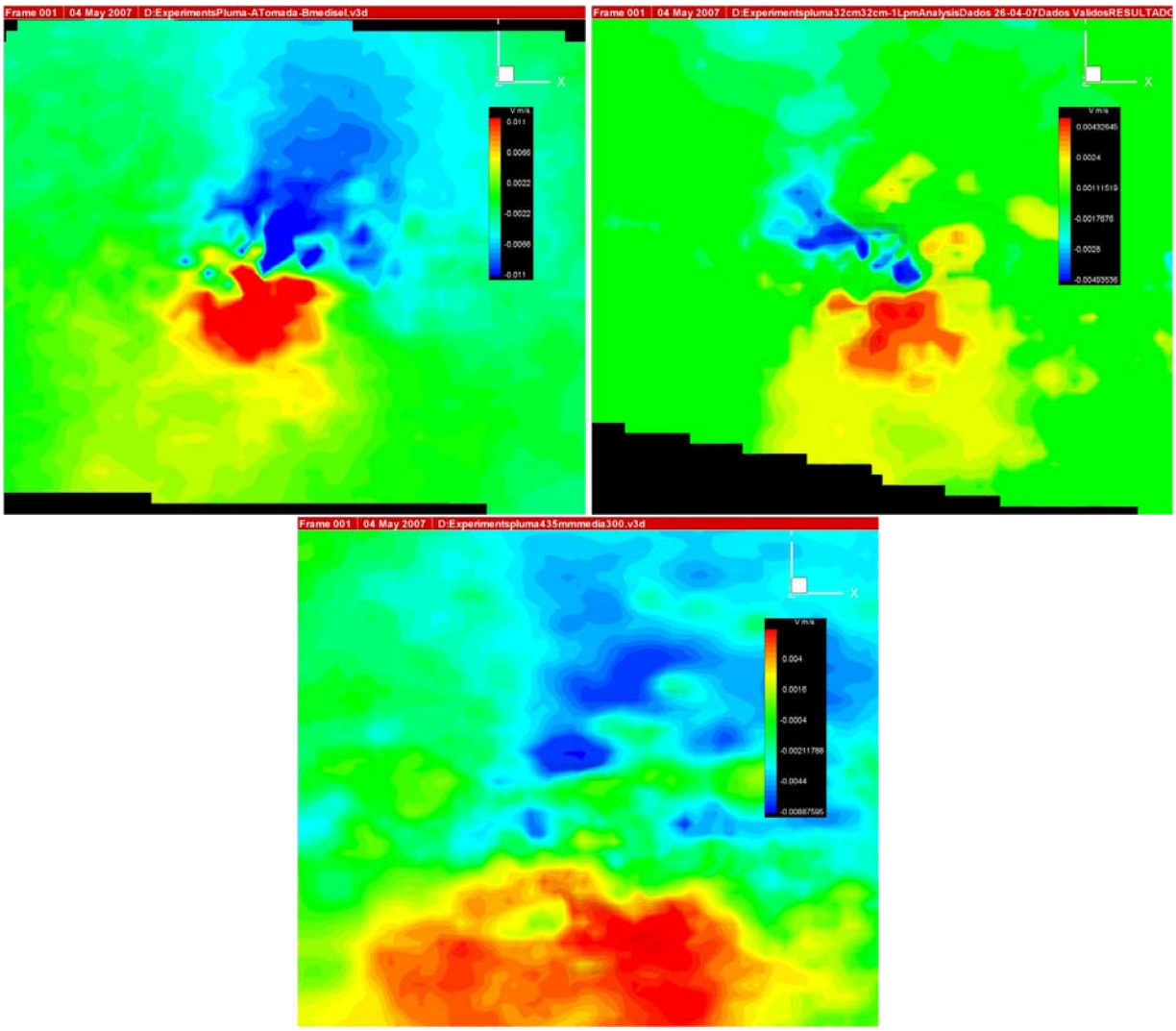

Figure 4. Entrainment velocities for the axisymmetric bubble plume at stations 235, 335 and 470 mm. Plane view.

velocities in the centerline. Therefore, as height increases the spread of the plume implies lesser values for the plume center velocity that, in turn, imply lesser values for the entrainment velocities.

The velocity profiles for the three dimensional bubble plume are shown in Fig. 6 for one z-stations, 470 mm. Note that the departure from a Gaussian profile is marked. The plume is clearly distorted toward the wall. The peak of maximum velocity is located near the wall and the velocity profile assumes a shape that is steep near the wall. This region is followed by a plateau of nearly constant velocity and a region velocity decay.

The entrained velocities are shown in Fig. 7. Contrary to Fig. 5, we observe that the entrainment velocities are definitively non-symmetric. Far away form the wall ($Y >$ - 65 mm) the entrainment velocities are nearly constant varying around v = - 0.008 ms^{-1}. Up to Y = - 85 mm, v suffers a large increase in magnitude reaching the value v = - 0.012 ms^{-1}. From this point on the entrainment velocity decreases steadily in magnitude tending to v = 0.0 at the wall.

Figure 7 gives a strong support to Eq. (11). Further data processing is currently under way so that the hypothesis of a varying entrainment coefficient can be investigated in much more detail.

6. Final remarks

The present work has shown that PIV measurements are indeed a resourceful means to find liquid phase velocities in bubble plume problems. The results confirm that the entrainment velocity suffers a strong inhibition near the wall, suggesting that models that resort to this physical mechanism for their development have strong foundations. The work has been important in identifying some relevant features of the problem, furnishing three dimensional data for the mean velocity profiles. These results are now being compared with void fraction results to identify further common ground for the development of a theory based on the work of Silva Freire et al. (2002)

In future measurements, the authors intend to present data on flow unsteadiness. Because present measurements were

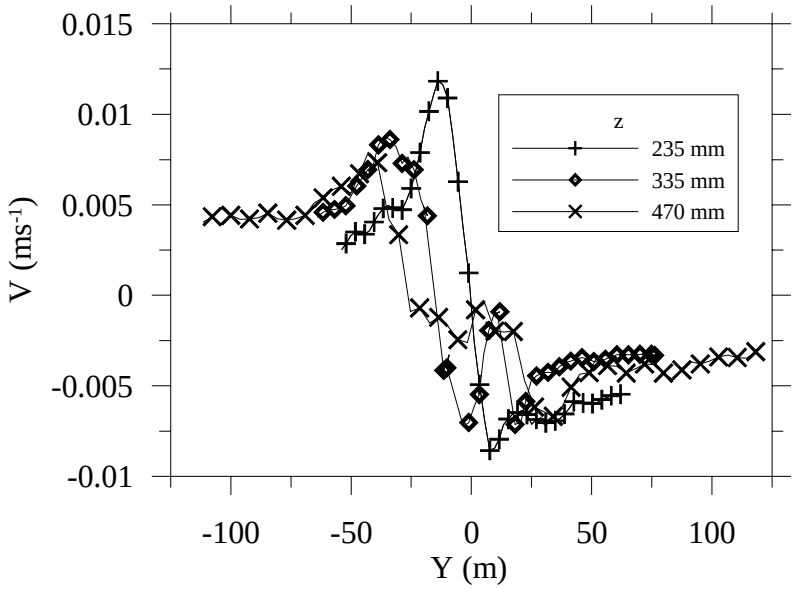

Figure 5. Entrainment velocities for the axisymmetric bubble plume along the Y-axis.

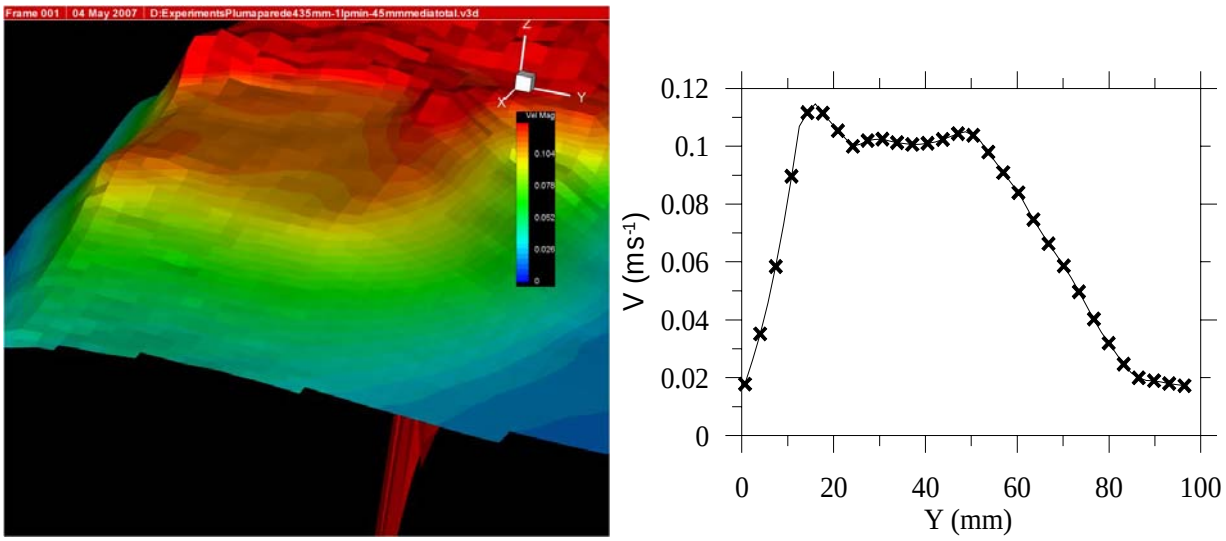

Figure 6. Flow topography of the 3D bubble plume including its non-Gaussian nature at station 470 mm.

mainly concerned with mean velocity data no wandering motion of the plume was reported. To the present authors' knowledge, this is the first time that the Coanda effect has been investigated in such detail. In particular, this is the first PIV study of such problem.

Acknowledgements. DGD benefited from a Research Scholarship from the Brazilian Ministry of Science and Technology through Programme Prometro. RP is grateful to CAPES for the award of a MSc scholarship. APSF is grateful to the Brazilian National Research Council (CNPq) for the award of a research fellowship (Grant No 304919/2003-9). The work was financially supported by CNPq through Grant No 472215/2003-5 and by the Rio de Janeiro Research Foundation (FAPERJ) through Grants E-26/171.198/2003 and E-26/152.368/2002.

7. References

Asai, S., Okamoto, T., He, J.C. and Muchi, I. , 1983, Trans. Iron Steel Inst. Jpn. 23, 43-50.

Barbosa, J. R. J. and Bradbury, L. J. S. 1996, Experimental Investigations in Round Bubble Plumes, In Proc. 6th Brazilian National Meeting on Thermal Sciences (ENCIT), Florianopolis, 1073-1078.

Brevik, I. and Killie, R., 1996, Phenomenological Description of the Axisymmetric Air-Bubble Plume, ,Int. J. Multiphase Flow, 22 535-549.

Castillejos, A. H. and Brimacombe, J. K., 1987, Measurement of Physical Characteristics of Bubbles in Gas-Liquid

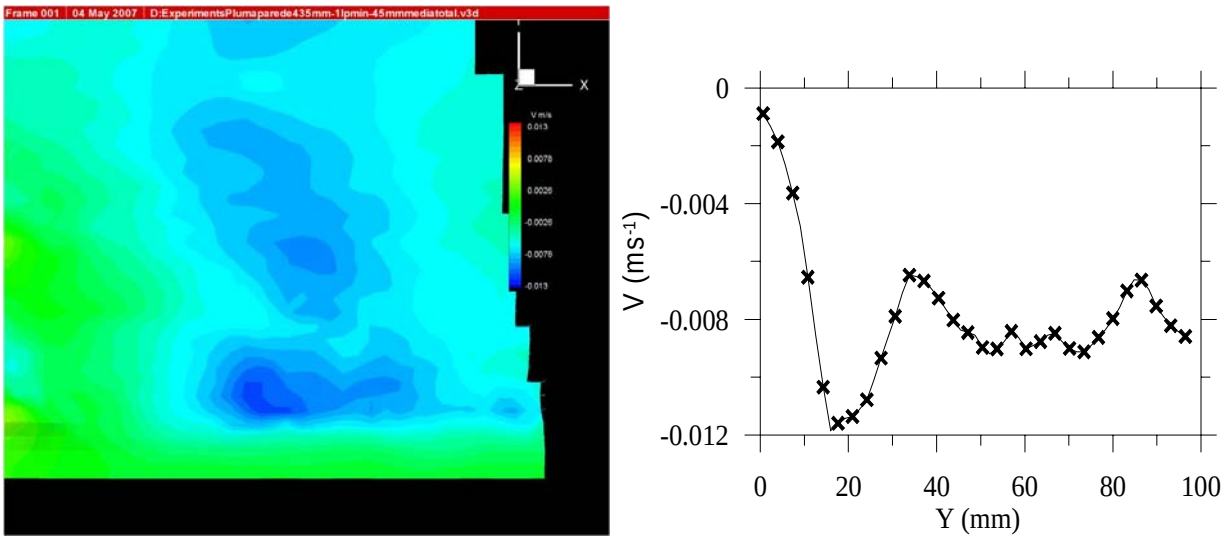

Figure 7. Entrainment velocities for the 3D bubble plume. Plane view and behaviour along the Y-axis.

Plumes, Metall. Trans. B, 18B, 649-671.

Ditmars, J. D. and Cederwall, K. 1974, Analysis of Air-Bubble Plumes, Proc. Coastal Engng Conf., Chap. 128, 2209-2226.

Dobson, C. J. and Robertson, M., 1988, Model studies for gas stirred ladles, Internal Report, BHP Steel, Australia.

Hassan, Y. A., Schmidt, W. D., Ortiz-Villafuerte, J., 1998, Investigation of three-dimensional two phase flow structure in a bubbly pipe flow, Meas. Sci. Technol., 9 309-326.

Joo, S. and Guthrie, R. I. L. 1992 Modeling Flows and Mixing in the Steelmaking Laddles Designed for Single- and Dual-Plug Bubbling Operations, Metall. Trans. B, No. 23B, 765–778.

Kim, S., Fruehan, R. J. and Guthrie, R. I L., 1987, Steelmaking Proc., ISS-ASME, Pittsburg, 107-10

Kline, S. J., 1985, The Purpose of Uncertainty Analysis, J. Fluids Engineering, 107 153-160.

Kobus, H. E., 1968, Analysis of the Flow Induced by Air-Bubble Systems, Proc. 11th Coastal Engng Conf. London, 2, Chap. 65, 1016-1031.

Lindken, D. and Merzkirche, W., 2000, Velocity measurements of liquid and gaseous phase for a system of bubbles rising in water, Exp. Fluids, S194-S201.

Majurama, T., Namishima, N. and Mizushina, T., 1984, J. Chem. Eng. Japan, 17, 120-126.

Mazumdar, R. and Guthrie, R. I. L., 1995, The physical and mathematical modelling of gas stirred ladle systems, ISIJ International, 35 1-20.

Menut, P. P. M., Barbosa Jr., J. R. and Silva Freire, A. P., 1998, 6o Brazilian Nat. Meeting on Thermal Sciences (6o ENCIT).

Milgram, J. H., 1983, Mean Flow in Round Bubble Plumes, J. Fluid Mech., 133 345-376.

Pera, L. and Gebhart, B. 1975 Laminar Plume Interactions, J. Fluid Mech., No. 68.

Reba, I. 1966 Applications of the Coanda Effect, Sci. Am., No. 214, 84–92.

Silva Freire, A. P., Miranda, D'E., Luz, L. M. S. and França, G. F. M, 2002, Bubble plumes and the Coanda effect, Int. J. Multiphase Flow, 28 1293-1310.